High speed movies of turbulence in Alcator C-Mod

J. L. Terry[a)]
Plasma Science and Fusion Center, MIT, Cambridge, Massachusetts 02139

S. J. Zweben
Princeton Plasma Physics Laboratory, Princeton, New Jersey 08543

B. Bose
Plasma Science and Fusion Center, MIT, Cambridge, Massachusetts 02139

O. Grulke
MPI for Plasma Physics, EURATOM Association, Greifswald, Germany

E. S. Marmar
Plasma Science and Fusion Center, MIT, Cambridge, Massachusetts 02139

J. Lowrance, V. Mastrocola, and G. Renda
Princeton Scientific Instruments, Inc., Princeton, New Jersey 08852

(Presented on 21 April 2004; published 13 October 2004)

A high speed (250 kHz), 300 frame charge coupled device camera has been used to image turbulence in the Alcator C-Mod Tokamak. The camera system is described and some of its important characteristics are measured, including time response and uniformity over the field-of-view. The diagnostic has been used in two applications. One uses gas-puff imaging to illuminate the turbulence in the edge/scrape-off-layer region, where D_2 gas puffs localize the emission in a plane perpendicular to the magnetic field when viewed by the camera system. The dynamics of the underlying turbulence around and outside the separatrix are detected in this manner. In a second diagnostic application, the light from an injected, ablating, high speed Li pellet is observed radially from the outer midplane, and fast poloidal motion of toroidal striations are seen in the Li^+ light well inside the separatrix. © *2004 American Institute of Physics.*
[DOI: 10.1063/1.1789597]

I. INTRODUCTION

Time sequences of two dimensional (2D) images ("movies") have been used extensively as plasma diagnostics for a long time; see e.g., Refs. 1 and 2. As the capabilities of imaging technology have increased, the range of diagnostic applications has increased apace, so that, as we report here, this technology is now being used to study phenomena that occur on ~1 μs timescales for periods of ~1 ms. One area where this type of imaging has been used productively and has great potential is in the imaging of plasma turbulence. Of course there is no well-defined boundary between arrays of "single-channel" views[3] and "cameras" with pixel arrays that are readout as "movie" frames. Generally, the more pixels there are in the 2D array the more "camera-like" is the diagnostic. Also, if the 2D array of pixels is built into a single detector or chip [e.g., a charge coupled device (CCD)], then it is usually considered a camera. In this case it is typical that the more pixels there are, then the slower the frame rate and/or the fewer the total number of sequential frames. In this article we report on a special CCD-based camera system that is capable of recording 300 64×64 pixel frames at a maximum 250 kHz frame rate. We also report on two diagnostic applications in which this camera system has been used: the study of edge turbulence and the study of pellet ablation in the high temperature plasmas of the Alcator C-Mod Tokamak.[4]

II. THE CAMERA SYSTEM AND "GAS PUFF IMAGING" OF TURBULENCE

The "ultrafast" camera was designed and built by Princeton Scientific Instruments.[5] In addition to its 250 kHz (maximum) frame rate and 64×64 array size, some of its other characteristics are: 65 μm $\times$ 195 μm pixels on a square grid with 202 μm spacing, ~18% quantum efficiency[6] (at 656 nm), low readout noise level (~20e), and 14 bit digitization. The 300 image frames are stored "on-board" using a chip architecture in which a CCD-type, charge-storage memory array is associated with each "active" photodetecting pixel. As each frame is registered, the charge packets from previous frames are shifted sequentially in these memory registers. When image acquisition is stopped, then the memory registers are clocked out at a much slower rate (~10 s) in order to minimize electronic readout noise. This architecture circumvents the usual low-frame rate limitation of high-density pixel arrays. This is the latest in a series of ultrafast cameras built by PSI and based on this architecture. In the following application an intensifier is used in front of the camera.

a)Electronic mail: terry@psfc.mit.edu

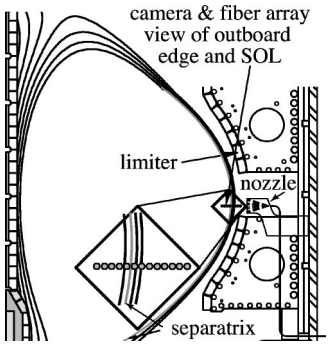

FIG. 1. (Color online) Schematic side view of the GPI system, including diamond-shaped field-of-view of camera and 13 focal spots of diode array views. Gas is puffed from a four-barrel nozzle at the right.

We have set up the camera to view light emission from the outboard midplane of C-Mod. The emitting atoms are supplied by a four-barrel nozzle that is located close to the plasma edge and through which D_2 or He is puffed. There is considerable fluctuation in measured emission, with the rms levels (normalized by the time average) typically exceeding 50% in some regions. The emission fluctuations are a result of the underlying turbulent fluctuations in plasma electron density and temperature, not the result of fluctuations in the gas flow. The local atom source results in toroidally localized emission that is viewed along tangential (and toroidal) chords by in-vessel optics. The technique is called "gas-puff imaging" (GPI), and is described in greater detail in Refs. 7 and 8. The schematic setup is shown in Fig. 1. A $\sim$6 cm $\times$6 cm diamond-shaped region of plasma edge/scrape-off-layer (SOL) in front of the nozzle is imaged onto a coherent fiber bundle, with the image transmitted via the bundle to the focal plane of a high quality camera lens. The light from the bundle is rendered parallel by that lens, filtered for the desired emission line by an interference filter, and then reimaged onto an image intensifier mounted on the front of the camera. The in-vessel optical system for the fiber bundle views along sight lines that are at an 11° angle with respect to horizontal. The combinations of lenses outside the vacuum are chosen so that the bundle image "fills" the camera chip area. The 11° in-vessel camera sight line was chosen so that it is nearly parallel to the local magnetic field for typical operation.

Two key characteristics of the camera system are its time response and it spatial uniformity. These qualities were measured. The time response to 4 and 1 μs light pulse is shown in Fig. 2. The measurement shows that time response of the camera/intensifier system is set mainly by the 250 kHz frame rate, not by the intensifier phosphor, P-46, which may have a $\sim$100 μs decay time from the 10% to 1% level. That effect is not seen here, at least for the signal-to-noise level and dynamic range typical in the experiment. We have also measured the response of the combined camera, intensifier, and fiber bundle system to a spatially uniform, constant-in-time source. If the average signal across the field-of-view is defined to be 1.0, then there is a systematic variation of local signal from a maximum level of 1.12 to values around 0.80.

In addition to the camera's view of the gas puff, there exists a 13-fiber array of single fiber views that views the gas

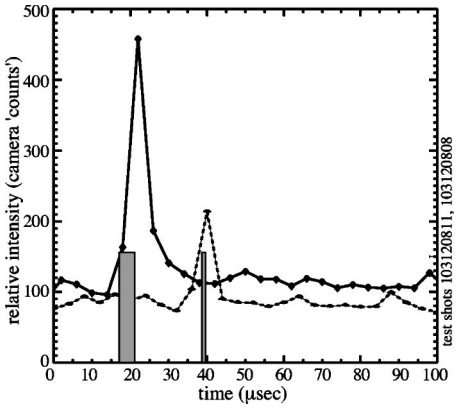

FIG. 2. Time response of the intensifier/camera system to flashes of 1 μs (dashed) and 4 μs duration (solid). The exact timings of the flashes within the camera's 4 μs sample times are not known, but are indicated by the shaded boxes.

puff region along purely toroidal chords, i.e., horizontally. These views are focused to $\sim$4 mm spots in front of the nozzle and are displaced radially from one another, but are aligned at the same vertical height; see Fig. 1. Light focused onto each fiber is brought to one of 13 photodiodes, interference filtered in the same way as the camera.[7] Thus the focal spots of the diode array views are included within the view of the camera, albeit with the viewing angle differing by 11°.

As an additional check on the performance of the system, we compare the time histories of the diode array signals with those from the pixels nominally focused on the same region. Two examples of this comparison are shown in Fig. 3. Typically, for most of the array views, the correlation between the camera signal and that of the diodes is quite high with cross-correlation coefficients from 0.65 to 0.9, e.g., as seen in Fig. 3. However there are discharges where the time history correlation is not good on some of the views. The reasons for this are still unknown. One difference is the 11° difference in viewing angles, although it is difficult to see how that can account for these occasional discrepancies.

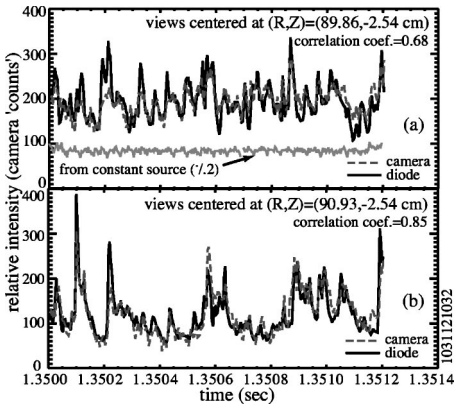

FIG. 3. (Color online) Emission time histories from two diode views of the diode array (solid) are compared with the time histories from the appropriate regions of the camera's field-of-view (grey-dashed). The measured emission is D_α during the same period of *H*-mode confinement. The spatial regions that are being compared are shown as black circles in Fig. 4. Also shown in (a) is the time history of emission from a steady-state source as detected by the same group of camera pixels used in the comparison with the diode signal.

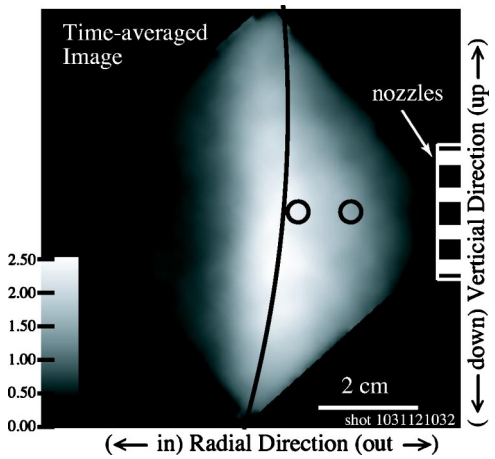

FIG. 4. (Color online) The 300 frame (1.2 ms) average image of D_α emission during a period of *H*-mode confinement. D_2 was puffed through the nozzle. Also shown are the location of the magnetic separatrix (solid black line), the location of the four-barrel gas-puff nozzle, and two of the 13 diode-array focal spots.

Also shown in Fig. 3(a) is the time history of the detected signal from a steady state source yielding a time-averaged signal level similar to the plasma source signal, i.e., ~160–200 counts. Note that, compared to the other frames, the steady state source signal level is systematically 10%–15% higher for the initial and final ~12 frames and that there is a systematic fixed-frequency variation from some of the pixel regions.

Using the system described above, movies of edge/SOL turbulence as manifested in the GPI emission were recorded for 1.2 ms at a 250 kHz frame rate. An example of a time-averaged emission pattern of D_α is shown in Fig. 4. The diamond shaped view of the region in front of the gas puff shows that the average emission straddles the separatrix in this *H*-mode confinement case. The average emission pattern is "windowed" radially by atomic physics, limited on the hot side by ionization and on the wall side by lack of excitation. The limits at top and bottom are set by the gas flow from the nozzle.

Cross-field particle transport in the SOL of tokamaks is typically strongly intermittent and convective (see Ref. 9 and references therein). It is primarily driven by the turbulence, with the larger amplitude events responsible for a large fraction of the transport.[10] Indeed, the camera movies show clear birth and motion of isolated regions of strong emission, six consecutive frames of which are shown in Fig. 5. These moving regions of strong emission are almost certainly the large amplitude ion-saturation current and floating-potential events seen on probes. They are typically called "blobs" in the literature, an appropriate name given the images. These kinds of image sequences serve as the raw material for analyses that attempt to measure things about the underlying turbulence and transport. For example, the long duration movies allow tracking of the turbulent structures as they propagate and statistical analyses of velocities, sizes, and "birth'' locations. They also can be compared with the predictions of turbulence simulation codes once the atomic physics of the gas puff is included.

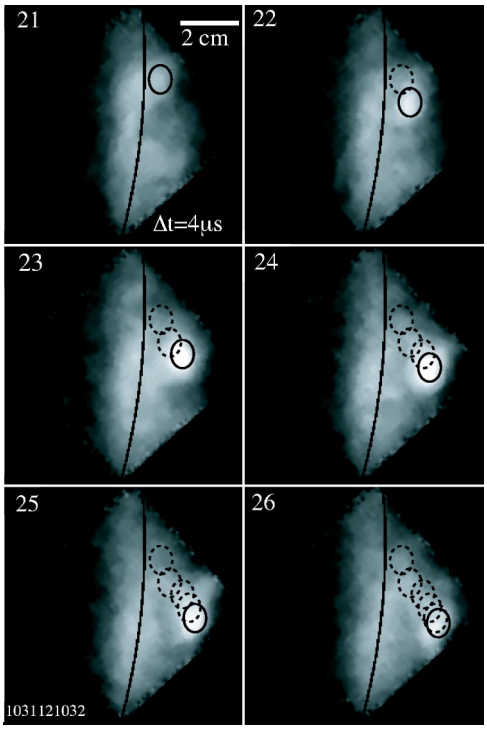

FIG. 5. (Color online) Six consecutive individual frames from the movie whose average emission is shown in Fig. 4. The birth and trajectory of a "blob" is clearly seen. The solid-line oval locates the position of the "blob" in the given frame, while the dashed-line ovals locate its positions in previous frames. This kind of intermittent event is typical, with many seen in one 300-frame movie.

III. CAMERA MOVIES OF PELLET ABLATION

The camera and earlier versions of the camera based on the same chip architecture have also been used in a completely different application, i.e., imaging ablation emission from high speed Li pellets injected into the high temperature plasma. The pellets are injected radially from the outboard side of the tokamak. They are imaged from behind their trajectory, i.e., by viewing radially inward. As the pellet penetrates the plasma, it ablates, and the ablatant ionizes rapidly. The ablated Li^+ is constrained in its movement perpendicular to the magnetic field, but is free to move along the field. Thus the Li^+ line emission (548.5 nm) is observed to have a cigar shape in the experimental viewing geometry with the long dimension of the "cigar" image aligned with the local magnetic field. A single frame showing a tilted, cigar-shaped main image (i.e., the one that includes the pellet nucleus) is displayed in Fig. 6. This 2 μs movie frame was measured by

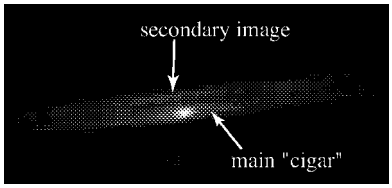

FIG. 6. (Color online) A single frame showing Li^+ line emission from an ablating Li pellet. As seen there is a bright central nucleus with a cigar-shaped emission cloud that is aligned with the local magnetic field. Of special interest is the dimmer emission cloud that is displaced poloidally, relative to the main cloud.

an earlier version of the camera that is capable of a 1 MHz frame rate, but is limited to 28 frames. Since the Li^+ ionizes in a time short compared to the pellet's radial motion, time resolved measurements of the "cigar" tilt can yield the radial profile of the pitch of the local field, and hence the plasma current profile.[11] The measurement of this tokamak parameter is of crucial importance, especially in the "advanced tokamak," or profile-controlled scenarios.

Another feature evident in the image of Fig. 6 is a dimmer cigar image displaced above the main image. This secondary image is frequently seen, but is seen in the movies to move rapidly in the poloidal dimension and to exist either *above or below* the main image at different times during the ablation. This has led to the speculation that the displacement of the secondary image is related to local, rapidly changing plasma flows, perhaps to the zonal flows that are predicted theoretically and are theoretically important to plasma transport. This speculation is currently being studied by the movies provided by the cameras.

IV. DISCUSSION

There are many other possible applications in plasma physics for this camera. The 1.2 ms duration of the time window allows for capture of other transient events. For example, an *L*-to-*H* mode transition can be observed by triggering the camera relative to the timing of additional auxiliary heating power. Also the dynamic effects of edge -localized -modes (ELMs) on the edge emission can be studied as long as the signal from an ELM precursor or trigger (e.g., a sawtooth crash) can be supplied. The view of the camera can be modified in a number of interesting ways, e.g., with larger or smaller magnification of the plasma viewing optics, or to view different regions of the edge/SOL. The magnification changes vary the range of turbulence size scales that can be observed, while different plasma regions almost certainly have different turbulence characteristics, e.g., at the inboard side or at the X point. We plan also to use the camera to view the plasma termination brought about by high-pressure impurity gas injection.

ACKNOWLEDGMENTS

This work is supported by DOE Cooperative Agreement No. DE-FC02-99-ER54512 and Contract No. DE-AC02-76CHO3073.

[1] D. J. H. Goodall, J. Nucl. Mater. **111–112**, 11 (1982).
[2] S. J. Zweben and S. S. Medley, Phys. Fluids B **10**, 2058 (1989).
[3] G. R. MCKee *et al.*, Rev. Sci. Instrum. **70**, 913 (1999).
[4] I. H. Hutchinson *et al.*, Phys. Plasmas **1**, 1511 (1994).
[5] Princeton Scientific Instruments, Inc., 7 Deer Park Drive, Monmouth Junction, N.J. 08852 ⟨www.prin-sci.com⟩
[6] This effective QE includes the fact that only 1/3 of the chip area is covered by "active" photodetector pixels. The *QE* for a given photodetector is $\times 3$ higher.
[7] J. L. Terry *et al.*, J. Nucl. Mater. **290**, 757 (2001).
[8] R. J. Maqueda *et al.*, Rev. Sci. Instrum. **72**, 931 (2001); S. J. Zweben *et al.*, Phys. Plasmas **9**, 1981 (2002); and R. J. Maqueda *et al.*, Rev. Sci. Instrum. **74**, 2020 (2003).
[9] B. LaBombard *et al.*, Phys. Plasmas **8**, 2107 (2001); and J. A. Boedo *et al.*, *ibid.* **8**, 4826 (2001).
[10] D. L. Rudakov *et al.*, Plasma Phys. Controlled Fusion **44**, 717 (2002).
[11] E. S. Marmar and J. L. Terry, Rev. Sci. Instrum. **61**, 3081 (1990).